J Mater Sci: Mater Med (2011) 22:629–636
DOI 10.1007/s10856-011-4231-9

In vitro adhesion of staphylococci to diamond-like carbon polymer hybrids under dynamic flow conditions

Antti Soininen · Jaakko Levon · Maria Katsikogianni · Katja Myllymaa · Reijo Lappalainen · Yrjö T. Konttinen · Teemu J. Kinnari · Veli-Matti Tiainen · Yannis Missirlis

Received: 22 October 2010 / Accepted: 4 January 2011 / Published online: 18 January 2011

Abstract This study compares the ability of selected materials to inhibit adhesion of two bacterial strains commonly implicated in implant-related infections. These two strains are *Staphylococcus aureus* (S-15981) and *Staphylococcus epidermidis* (ATCC 35984). In experiments we tested six different materials, three conventional implant metals: titanium, tantalum and chromium, and three diamond-like carbon (DLC) coatings: DLC, DLC–polydimethylsiloxane hybrid (DLC–PDMS-h) and DLC–polytetrafluoroethylene hybrid (DLC–PTFE-h) coatings. DLC coating represents extremely hard material whereas DLC hybrids represent novel nanocomposite coatings. The two DLC polymer hybrid films were chosen for testing due to their hardness, corrosion resistance and extremely good non-stick (hydrophobic and oleophobic) properties. Bacterial adhesion assay tests were performed under dynamic flow conditions by using parallel plate flow chambers (PPFC). The results show that adhesion of *S. aureus* to DLC–PTFE-h and to tantalum was significantly ($P < 0.05$) lower than to DLC–PDMS-h ($0.671 \pm 0.001 \times 10^7/\text{cm}^2$ and $0.751 \pm 0.002 \times 10^7/\text{cm}^2$ vs. $1.055 \pm 0.002 \times 10^7/\text{cm}^2$, respectively). No significant differences were detected between other tested materials. Hence DLC–PTFE-h coating showed as low susceptibility to *S. aureus* adhesion as all the tested conventional implant metals. The adherence of *S. epidermidis* to biomaterials was not significantly ($P < 0.05$) different between the materials tested. This suggests that DLC–PTFE-h films could be used as a biomaterial coating without increasing the risk of implant-related infections.

Antti Soininen and Jaakko Levon contributed equally to this work.

A. Soininen (✉) · Y. T. Konttinen · V.-M. Tiainen
ORTON Research Institute of the ORTON Orthopaedic Hospital, Tenholantie 10, 00280 Helsinki, Finland
e-mail: antti.soininen@orton.fi

J. Levon · Y. T. Konttinen
Department of Medicine, Helsinki University Central Hospital, Helsinki, Finland

M. Katsikogianni · Y. Missirlis
Laboratory of Biomechanics and Biomedical Engineering, Department of Mechanical Engineering & Aeronautics, University of Patras, Patras, Greece

K. Myllymaa · R. Lappalainen
Department of Physics, University of Kuopio, Kuopio, Finland

Y. T. Konttinen
COXA Hospital for Joint Replacement, Tampere, Finland

T. J. Kinnari
Department of Otolaryngology, Helsinki University Central Hospital, Helsinki, Finland

1 Introduction

Infections associated with biomedical devices have serious consequences for the patients and inevitably increase costs to the society. Bacterial adhesion, colonization, and subsequent formation of resistant biofilms on an implant surface are the major reasons for implant-related infections of orthopedic implants [1–5]. These infections can usually be cured only by device removal, with antibiotics being used as a supportive therapy and for eradication. Because *Staphylococcus aureus* and *Staphylococcus epidermidis* are the most common causative pathogens associated with implant-related infections, these two bacteria were selected for probing of materials of interest [6–8]. As the implant or coating designed for clinical use will be subjected to body fluid flow, bacterial adhesion should be studied under

dynamic rather than static conditions. Many staphylococcal infections spread hematogenously via circulation, where wall shear rate ranges between 40 and 2000 s^{-1} for stable Poiseuille flow vessels [9]. Static and low shear rate conditions lead to bacterial aggregation due to the long intercellular contact time. Adhesion of *S. epidermidis* to different biomaterials does not vary under static conditions or at shear rates <50 s^{-1}, whereas biomaterial differences become evident at a shear rate of 200 s^{-1} [10]. On the other hand, when too high shear rates are used, adhesion of *S. epidermidis* to materials decreases because hydrodynamic forces predominate [11]. The same phenomenon is seen for *S. aureus* when shear rate exceeds 300 s^{-1} [12, 13]. Because we wanted to avoid artifacts caused by low shear rates and study the effect of biomaterial properties on bacterial adhesion and not their ability to withstand detachment (retention), 200 s^{-1} shear rate was used throughout the experiments.

One way to prevent implant-related infections is to use functional coatings, which are able to inhibit microbial adhesion. Many groups, including us, have studied protective wear and corrosion resistant diamond-like carbon (DLC) coatings [14–16]. To combine useful properties of DLC and polymers, the filtered pulse arc discharge (FPAD) technology developed in our laboratory to produce high-quality DLC coatings was modified to produce novel DLC polymer hybrid (DLC–p-h) coatings. Two novel nanocomposite hybrid coatings were prepared for testing: DLC polytetrafluoroethylene hybrid (DLC–PTFE-h) and DLC polydimethylsiloxane hybrid (DLC–PDMS-h). A priori, both these materials are promising candidates to medical implant applications due to their extremely good non-stick (i.e. hydrophobic and oleophobic) properties [17–19]. Our hypothesis was that these hard, anti-soiling and non-stick coatings could be better or as good as conventional DLC coating and/or conventional implant materials in their ability to resist bacterial adhesion under dynamic flow conditions. Because bacterial adhesion susceptibility of surgical steel (AISI 316L) versus DLC was already tested in earlier experiments [20] three other commonly used materials in medical devices were selected for testing: tantalum, titanium and chromium.

2 Materials and methods

2.1 Coating methods and sample preparation

Tantalum, titanium, chrome, DLC, DLC–PDMS-h and DLC–PTFE-h coatings were deposited on monocrystaline {100} silicon wafers (Okmetic, Vantaa, Finland). Silicon wafers used were 101.6 mm in diameter and 0.68 mm in thickness. Deposition of the coatings was done by utilizing two different deposition methods, a direct current (DC) sputtering technique for metals (titanium, tantalum and chrome) and a filtered pulsed arc discharge (FPAD) method for DLC and DLC polymer hybrid films (DLC, DLC–PTFE-h and DLC–PDMS-h). These two deposition methods have been described in detail elsewhere in the literature [21–25]. Some relevant features and parameters of the techniques as applied in the present experiments are described below.

Before the deposition, all sample surfaces were cleaned with argon sputter (SAM-7 kV, Minsk, Belarus) in vacuum. The initial vacuum chamber pressure was 8×10^{-4} Pa. The sputtering time was 10 min and the voltage and current used were 5 kV and 30 mA, respectively. During the argon sputtering the vacuum chamber pressure was 0.01 Pa. The purity of argon was 99.999% (Instrument Argon 5.0, Oy AGA Ab, Espoo, Finland). All deposition processes were continued directly after the argon sputtering without breaking the vacuum.

In DC sputtering system (Stiletto Series ST20, AJA International Inc., North Scituate, MA, USA) a negative target potential of 500 V was used to accelerate the positively charged Ar ions to the high purity (99.7% or better) elemental metal target (Goodfellow Cambridge Ltd, Huntingdon, England). The deposition rate of metal to the sample surface was 40 nm per minute and deposition time was 5 min.

In FPAD system high purity graphite cathode (99.9%, Carbone Lorraine, Paris, France) or graphite-polymer (PDMS and PTFE tube, Irpola Oy, Turku, Finland) cathode construction were used to deposit DLC, DLC–PTFE-h or DLC–PDMS-h coatings, respectively. Deposition of DLC coatings was done in two steps. First an adhesion layer was deposited using high plasma energies and secondly the coating itself was deposited using a low energy FPAD system. First, high energy plasma was accelerated using a voltage of 5 kV with capacitor ($C = 16.0$ μF). The plasma was steered towards the sample with a magnetic field generated by the arc discharge current in a 90° curved solenoid ($L = 3.0$ μH). The curved solenoid filters out neutral atoms and graphite particles emitted from the cathode. The plasma accelerating cathode–anode pair, the solenoid, the tuning resistor ($R = 0.1$ Ω) and the main capacitor bank were all connected in series. The high-quality DLC coating was then deposited using low energy FPAD system. Low energy system parameters were: voltage $U = 0.5$ kV, solenoid $L = 20$ μH, capacitor $C = 30$ μF and tuning resistor $R = 0.1$ Ω. For DLC polymer hybrid coatings two different graphite cathodes with PDMS or PTFE tube were used. Deposition times were 15 min in all cases. The DLC coatings analyzed in this study were hydrogen free and amorphous [25, 26] with high diamond sp^3 bond content (85%) [27]. Recent AFM studies (not

published) of DLC–p-h coating surfaces indicate that mixing of DLC and polymer component occurs in nano-scale and, thus, different regions of diamond or polymer cannot be distinguished on the coating surfaces. The thickness of DLC, DLC–PDMS-h and DLC–PTFE-h samples was 150 ± 20 nm and thickness of tantalum, titanium and chrome layers was 200 ± 20 nm.

After the coating process the coated silicon wafers were cut using a custom-made diamond knife device to rectangular pieces (dimensions: 15 mm × 30 mm), which fitted perfectly in the bacterial flow testing chambers. The cutting apparatus was designed in such a way that it does not alter the surface chemistry or contaminate the samples during the cutting process.

2.2 Sample thickness and surface roughness analysis

Topography and thickness of the surfaces were examined with a 2D stylus profiler (Sloan Dektak IIa, Veeco Instruments Inc., Santa Barbara, California, USA). Sample thickness was measured from coated silicon wafers separately for each coating batch. This was done by placing a mask to the sample for the coating period, removing it after the coating process and measuring the step on the sample.

2.3 Contact and sliding angle measurements

Contact angle measurements were done using the static sessile drop method with a CCD video microscope and 20 μl distilled water droplets. The sliding angles were also measured with 20 μl distilled water droplets. The sliding angle is defined as the critical angle at which a droplet begins to slide down an inclined plane. The accuracy of a single contact or sliding angle measurement was ±0.5°.

2.4 Bacterial cultures

The bacterial strains used in this study were the reference type culture, slime producing *S. aureus* S-15981 strain and *S. epidermidis* ATCC 35984 strain. The *S. aureus* S-15981 is a clinical isolate from University of Navarra, Spain. It was isolated from middle ear exudates of a patient suffering from recurrent otitis media. The strain is resistant to gentamycin and sensitive to all other currently used antibiotics. It is a strong biofilm former and agr negative [28]. Microorganisms were kept at −70°C, in a solution containing 70% Tryptic Soy Broth (TSB, Difco Laboratories, Detroit, USA) and 30% diluted glycerol (glycerol/water: 1/1). In order to prepare the bacterial cells for the adhesion assays, 10 μl of the frozen bacterial suspension, of each strain, were cultured on blood agar plates overnight at 37°C and subsequently stored at 4°C. Stationary phase cells were obtained by incubating two to three colonies, from the blood agar plate, in 5 ml TSB for 18 h at 37°C in a rotary shaker at 120 rounds per minute. Bacterial cells were harvested by centrifugation at a centrifugal force of $2683 \times g$, at 4°C for 10 min, washed twice with a buffer, pH 7.4, ionic strength 180 mM, consisting of 100 mM phosphate buffered saline supplemented with 80 mM NaCl, and finally resuspended in the same buffer. The concentration was adjusted to 1.5×10^8 colony forming units (CFUs)/ml, by measuring the optical density of the bacterial suspension at wavelength of 550 nm with a spectrophotometer (Techne, Cambridge, UK), according to the McFarland standard (BioMerieux, SA Lyon, France).

2.5 Dynamic adhesion assays

For evaluation of bacterial adhesion under flow conditions the parallel plate flow chamber (PPFC) [29] was used. The 30 mm × 15 mm × 1 mm sample is sandwiched between two plexiglas plates in such a way that a 30 mm × 15 mm × 0.35 mm parallel plate flow chamber is formed. Four syringes were placed in an automated syringe pump and connected to four different chambers. The pump was programmed to cycle the pistons back and forth every 60 s continuously, at which time 3.7 ml were displaced. This cycle repeated itself for 120 min. All experiments were carried out at 37°C. The shear rate was adjusted to 200 s^{-1}. The shear rate γ can be calculated by the following formula:

$$\gamma = \frac{6Q}{Wh^2}$$

where Q is the flow rate, W (width of the chamber) = 15 mm and h (height of the chamber) = 0.35 mm. Each experiment was performed in three replicates.

2.6 Fixation and staining of adherent bacterial cells

After adhesion experiments, each sample was rinsed with 8 ml buffer solution to remove non-adherent or loosely adherent bacteria. At the next step the samples were fixed in freshly prepared 3% formaldehyde for 30 min at 37°C. Formaldehyde was prepared by adding paraformaldehyde (Sigma, Missouri, USA) in 100 mM sodium phosphate buffer at 60°C, followed by drop-wise addition of NaOH until the solution was clear. After fixation, the samples were stained in 1 ml of a freshly prepared solution containing 2 μl SYTO 9 (Molecular Probes, Europe BV) per 1 ml deionized water. Samples were kept in this diluted SYTO 9 solution for 30 min at room temperature, in the dark. The staphylococcal membrane penetrating SYTO 9 is a fluorescent DNA-binding stain and was used to visualize the distribution of adherent bacteria. After staining the samples were rinsed three times with distilled water, placed on an object slide and mounted in Gel Mount (Sigma,

Missouri, USA), that is an aqueous mounting medium. Finally, the samples were covered with a cover slip.

2.7 Microscopy, photographing and image analysis

Confocal microscopy was carried out to examine bacterial adhesion to the samples and to enumerate the adherent bacteria. For this purpose a Nikon TE2000-U Confocal Laser Scanning Microscopy (CLSM) system was used (Nikon, The Netherlands). The system consisted of a laser scanning module that was mounted on an inverted microscope. The argon laser was used and the images were recorded at an excitation wavelength of 488 nm and at an emission wavelength of 500 nm. Since the adherent bacteria were in a monolayer, a thin section was scanned and saved as a bitmap image. Six fields of 100 μm^2 area were chosen randomly and six non-overlapping images were taken from each sample to eliminate the eventual effect of slightly uneven distribution of bacteria. Digital image analysis of the CLSM images and the quantification of adherent bacteria were performed using the software developed at the University Medical Center Groningen, University of Groningen in The Netherlands. The software is based on the methods described earlier [30].

2.8 Statistical analysis

The effect of the material properties on bacterial adhesion was statistically analyzed using the SPSS statistical software, version 14.0 (SPSS, Chicago, IL). The normal distribution of the variables was examined using the Shapiro–Wilk (W) test. Since W was close to one for all variables, they were normally distributed. Afterwards, one way analysis of variance (ANOVA), and Post-hoc comparisons of all possible combinations of group means, were performed using the Scheffe significant difference test. $P < 0.05$ was considered to be significant.

3 Results

Quantitative analysis of bacterial adhesion was performed by confocal fluorescence laser scanning microscopy, digital image processing and image analysis software. This allowed the enumeration of the attached bacteria. Fig. 1a demonstrates the adhesion of *S. aureus* on different study materials, with one representative micrograph for three of the tested materials. DLC, titanium and chromium micrographs are not shown because they did not contain any additional information. The number of *S. aureus* bacteria on different materials, counted using an image analysis software, are shown in Fig. 2a in a bar diagram. The results show that adhesion of *S. aureus* to DLC–PTFE-h and to tantalum was significantly ($P < 0.05$) lower than to DLC–PDMS-h ($0.671 \pm 0.001 \times 10^7/cm^2$ and $0.751 \pm 0.002 \times 10^7/cm^2$ *vs.* $1.055 \pm 0.002 \times 10^7/cm^2$, respectively). No significant differences were detected between the other materials tested. Similarly, Figs. 1b, 2b demonstrate the results obtained for *S. epidermidis*. In Fig. 1 b) three chosen micrographs of DLC, titanium and chromium demonstrate similar adhesion of *S. epidermidis* to all materials. The results show that *S. epidermidis* adhered equally to all materials tested ($P < 0.05$).

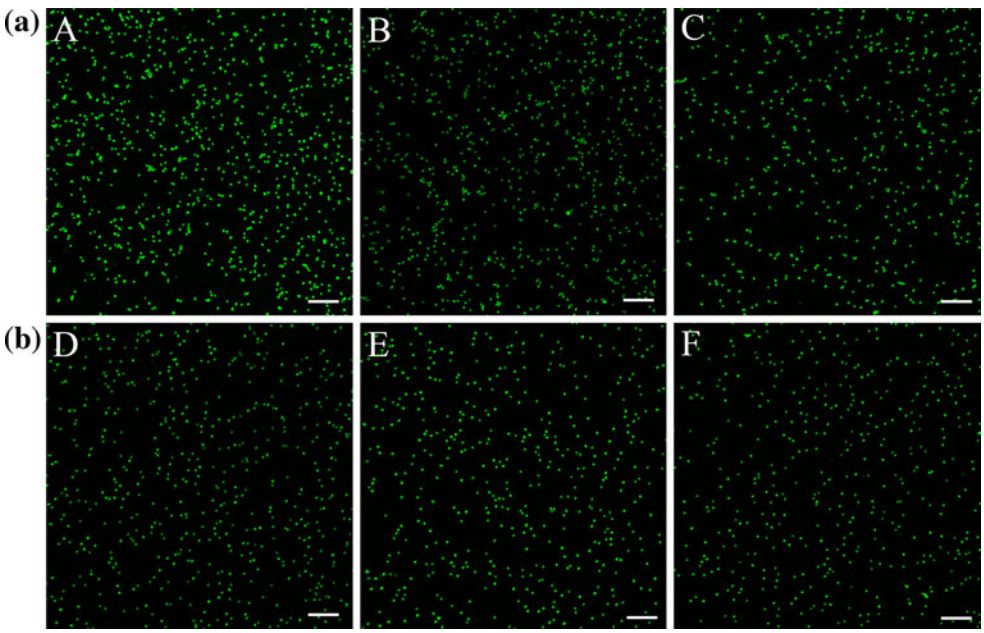

Fig. 1 Confocal fluorescence laser scanning microscopy micrographs of the material surfaces after 120 min dynamic bacterial adhesion tests. **a** *S. aureus* S-15981 to DLC-PDMS-h (*A*), DLC-PTFE-h (*B*) and tantalum (*C*). **b** *S. epidermidis* ATCC 35984 to DLC (*D*), titanium (*E*) and chromium (*F*). *Scale bar* 10 μm

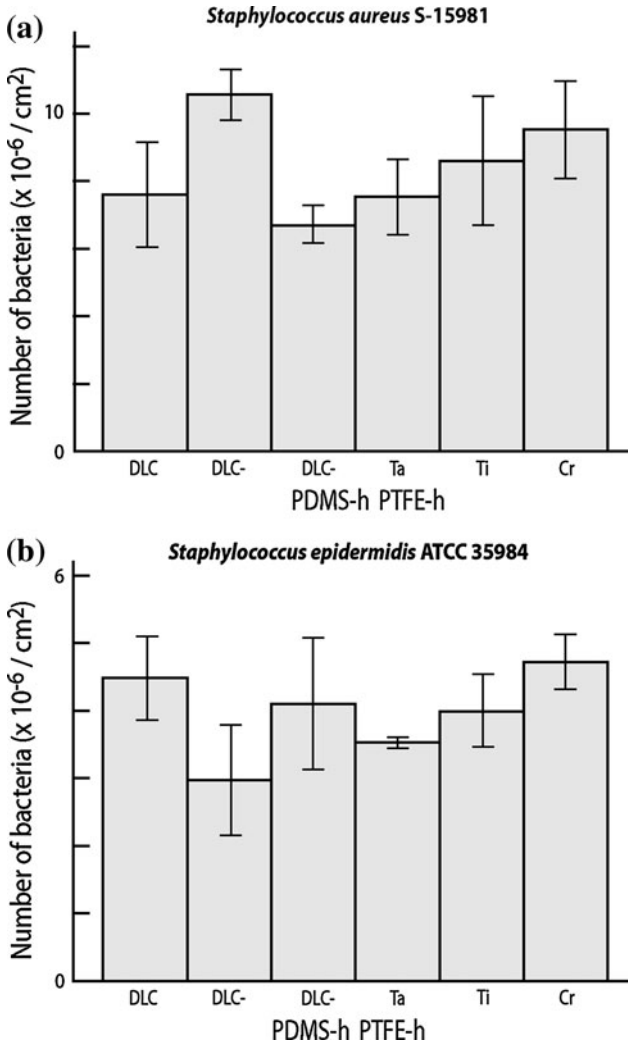

Fig. 2 Number of bacteria adhered on DLC, DLC–PDMS-h, DLC–PTFE-h, Ta, Ti and Cr surfaces after 120 min of dynamic bacterial adhesion test. **a** *S. aureus* S-15981 **b** *S. epidermidis* ATCC 35984

Surface roughness was analyzed to evaluate its eventual effect on bacterial adhesion. Roughness values (Ra) obtained using profilometry are presented in Table 1, and were 3 ± 2 nm for DLC, DLC–PDMS-h, DLC–PTFE-h samples and 17 ± 3 nm, 19 ± 3 nm and 25 ± 3 nm for tantalum, titanium and chrome samples, respectively. Surface roughness values (Ra) were determined with a 2D stylus profiler by scanning the length of 1 mm on the surface.

Contact and sliding angles were measured to evaluate the surface hydrophobicity of titanium, tantalum, chromium, DLC, DLC–PDMS-h and DLC–PTFE-h coatings. This analysis showed the highest contact angle values for DLC–PDMS-h and DLC–PTFE-h, which were 104 ± 4°, and the lowest sliding angle for DLC–PDMS-h, which was 9 ± 1°. All contact and sliding angle values are presented in Table 1.

4 Discussion

DLC coating used in this study has many properties which makes it a very desirable biomaterial coating: it is wear and corrosion resistant and at the same time biocompatible [14–16, 31–33]. Similarly, polymers used as additives in the deposition process of DLC, like polytetrafluoroethylene (PTFE) and polydimethylsiloxane (PDMS), have useful properties by being non-stick and anti-soiling [34–36]. FPAD system was modified to deposit coatings, where DLC and polymer components are combined. As a result, a whole new group of materials was produced: hard, hydrophobic and oleophobic DLC polymer hybrid (DLC–p-h) coatings. In these novel coatings the hardness of the DLC and the anti-soiling properties of the additive polymer are combined [17–19]. Thus by using this modified FPAD method it is possible to produce well-adherent DLC polymer hybrid coatings of novel biomaterials, in which the proportions and useful properties of the source materials can be combined in an innovative and purpose-designed manner. These non-stick and anti-soiling biomaterials could find applications in stents or mechanical heart valves, which even in warfarin treated patients can evoke thromboembolic complications. These DLC polymer hybrid coatings however have not been studied before in dynamic flow conditions for their ability to inhibit adhesion of *S. aureus* and *S. epidermidis*, which property should not be compromised by this new formulation. These bacteria are the most common causative agents in implant and medical device related infections and cause also infections of

Table 1 Contact angle, sliding angle and surface roughness (Ra) of the biomaterials tested in the present study

Coating	Contact angle (°)	Sliding angle (°)	Roughness, Ra (nm)
DLC	58 ± 1	70 ± 1	3 ± 2
DLC–PDMS-h	104 ± 4	9 ± 1	3 ± 2
DLC–PTFE-h	104 ± 4	40 ± 1	3 ± 2
Ta	21 ± 1	38 ± 1	17 ± 3
Ti	55 ± 2	*	19 ± 3
Cr	72 ± 2	*	25 ± 3

All contact and sliding angle measurements were done with 20 µl distilled water droplets. *Asterisks* denotes that droplet did not start to slide even at 90°

artificial heart valves. According to the present results, DLC–PTFE-h and DLC–PDMS-h are comparable, but not in this respect any better, to widely used metallic biomaterials and conventional DLC with one exception: DLC–PDMS-h bound more *S. aureus* than DLC–PTFE-h and tantalum, which were in the test setting used the most resistant to bacterial adhesion. It should be noted that bacterial adherence to DLC–PDMS-h was otherwise comparable with all the other tested materials and *Staphylococcus* strains. Under static conditions the new DLC–PTFE-h coating has been described to resist adhesion of two different staphylococcal strains better than titanium or oxidized silicon [31].

The three metals tested, tantalum, titanium and chromium, are commonly used metallic materials in medical devices. Because these three materials are metals, it is to be noted that they all are reactive and spontaneously form a thin, passive and stable surface oxide layer in open air and in liquids. However, similar oxide layers, responsible for the good corrosion properties of metallic biomaterials, form also on real implants. Therefore, we do not consider these oxide films as confounding factors in the present study.

Hydrophobic interactions have been used to explain bacterial adherence to surfaces. Hydrophilicity seems to reflect repellence capability, whereas hydrophobicity has been associated with bacterial adherence to the material surface. Shi and coworkers showed that mucin coating of polymethylmethacrylate, polystyrene and silicone increased their hydrophilicity and decreased bacterial adhesion [37]. Van Loosdrecht et al. [38]. reported that also the hydrophobicity of the bacteria (measured using water contact angle) increased adherence on negatively charged hydrophobic sulfated polystyrene, whereas hydrophilicity of microorganisms decreased bacterial adherence. Adhesion of nine clinical isolates of *S. epidermidis* to hydrophobic acrylic surfaces was higher than to hydrophilic glass surfaces [39]. In our experiments we used water contact angle measurements to evaluate the hydrophobicity of the studied materials. Among the conventional implant metals tested tantalum had the lowest contact angle being the most hydrophilic metallic biomaterial, followed by titanium, which was more hydrophobic than tantalum, and by chrome, which was the most hydrophobic of the metallic biomaterials tested. This ranking order is exactly the same as their ability to resist bacterial adherence in both *S. aureus* and *S. epidermidis* experiments, see Table 1 *vs.* Fig. 2 a, b). These findings are in favor of the above mentioned hydrophilicity axiom. However, when also DLC and DLC hybrid coatings are considered this co-ranking of hydrophilicity and bacterial repellence is lost. For example, DLC–PTFE-h and DLC–PDMS-h were the most hydrophobic materials with an equally high water contact angle, but DLC–PTFE-h coating was the most resistant to bacterial adherence of all the materials tested. In this study, contact and sliding angle studies were carried out to determine whether there was a relation between hydrophobic or hydrophilic property and bacterial adhesion. Results convincingly suggest that this physicochemical property does not appear to be the primary or only contributor which influences bacterial adhesion, even though the tested three conventional surgical metals seemed to follow the expected pattern. In general, uncapsulated staphylococci are hydrophobic and from this point of view, should stick better to hydrophobic than hydrophilic surfaces. As already mentioned above, this seems to hold true for the Ta, Ti and Cr and maybe even for DLC. It should also be taken into consideration that the relationship between adherence and hydrophobicity may be complex as has been shown for the relationship between adherence of bone marrow-derived mesenchymal stromal cells and hydrophobicity: these cells adhere better to materials with an intermediate contact angle than to more hydrophilic or hydrophobic surfaces. The turning point of this parabolic relationship for these cells is around the contact angle 60° [40]. Accordingly, one might think that the very hydrophobic surface (with low surface energy) of DLC–PTFE-h could explain why its *S. aureus* binding was very low. But even such a parabolic relationship cannot explain that DLC–PTFE-h had the lowest *S. aureus* binding ability whereas the DLC–PDMS-h surface with exactly the same contact angle (104°) had the highest ability to bind *S. aureus*. In this respect, the present observations are in accordance with the findings of Raulio et al. [41] and Jones et al. [42].

There seems to be other factors that affect the bacterial adhesion more than hydrophobicity and surface roughness evaluation can explain. It is known that the sp^3 and sp^2 hybridized carbon–carbon bond ratios in DLC materials affects its properties [25]. In these now tested novel DLC–p-h materials sp^3 and sp^2 bond ratios are not very well known yet. These unknown factors also include mechanical, optical and perhaps in particular electrical properties, such as the zeta-potential. In addition, experimental flow setting changes bacterial behaviour and its surface structures in such a way that the results between static and dynamic adhesion tests may be different, as seen in our work. This suggests that the bacterial adhesion test reports should include more extensive information on different material and microbial properties than is normally reported. Anyway, valuable observations have already been made regarding factors contributing to bacterial adhesion and biofilm formation. Objects of interest have been the conditioning of the surfaces, mass transport, hydrophobicity, surface roughness and molecular structures of the bacterial surface (surface proteins and teichoic acid)

through which the adhesion process is maintained [43]. When investigating a certain specific property, it is often difficult to obtain reliable information on other possible contributors or to disclose various confounding factors. Our study concentrated on the effect of dynamic flow environment, surface roughness and hydrophobicity on bacterial adhesion of two *staphylococcal* strains. At this time, there is no single straightforward explanation for our results, but they might relate to the sp^3 and sp^2 ratio and zeta-potential. Microbe-material interaction is a complex event, thus, experimentation under different conditions is the only way to assess it.

Bacterial adhesion leads to formation of a biofilm, where bacterial cells are embedded in mucopolysaccharide extracellular matrix. On device surfaces biofilm formation protects the living bacterial cells from the antimicrobial drugs and host defense molecules as well from leucocytes. This explains why implant-related infections are difficult to eradicate without removal of the implant. Most bacterial in vitro adhesion studies have for practical reasons been done under static conditions. However, in vivo bacteria and biofilms are usually subjected to shear forces of the human body fluids. The best primary prophylaxis against infections would be to use biomaterials or coatings able to inhibit bacterial adhesion. Previously our group has performed static adhesion studies with traditional prosthesis materials and DLC. Under the conditions used the following ranking order was achieved using adhesion index: titanium, tantalum, chromium and DLC, with the DLC being clearly most resistant against colonization with *S. aureus* [44]. In our current study under flow conditions there were no significant differences between DLC and the other materials previously tested. Thus, it seems that for full scale comparison of the ability of different materials to inhibit bacterial adhesion not only the static but also the dynamic conditions should be tested. The last mentioned conditions more closely mimic those prevailing in vivo.

Contact angles of DLC, DLC–PDMS-h and DLC–PTFE-h did not correlate with their sliding angles. For example, both DLC polymer hybrids had the same contact angle, but the sliding angle was very different. This is in accordance with earlier findings of Kiuru and Alakoski [19] and Chen et al. [45]. Present results also indicate that the difference in bacterial adherence between DLC–PMDS-h vs. DLC–PTFE-h or tantalum cannot be explained by differences between their contact and sliding angles (hydrophobicity).

The surface roughness values of the biomaterial samples tested were not quite identical although they had a very narrow range between 2 and 25 nm. It has been earlier reported that at least for surgical steel (AISI 316L) [46] and polymethylmethacrylate (PMMA) [47] differences in the surface roughness of this order do not affect bacterial adherence although larger differences in the one micron range, corresponding to the size of the bacteria, do affect adherence. Therefore, the slight differences in the surface roughness of the samples tested do not form a confounding factor and cannot explain the differences in bacterial adherence between DLC–PMDS-h *vs.* DLC–PTFE-h or tantalum.

In conclusion, the novel DLC–PTFE-h coating was comparable to conventional DLC coating and to three common metallic materials used in medical devices in this dynamic bacterial adhesion test setting. Results also indicate that DLC–PTFE-h coating and tantalum inhibit *S. aureus* adherence slightly better than the DLC–PDMS-h coating. No differences were detected between other tested materials and staphylococcal strains. These results suggest that utilization of DLC–PTFE-h coating in medical devices and operating theatres, due to its other interesting properties, such as anti-soiling and non-stick properties, could be done without increasing the risk of infections.

Acknowledgments This research work has been supported by Sigrid Jusélius Foundation, ORTON evo-grant, ORTON Foundation, European Science Foundation "Regenerative Medicine" RNP, the Danish Council for Strategic Research "Individualized Musculoskeletal Medicine", MATERA project "RSHI-DLC-nanocomp". PhD-programme in Musculoskeletal Diseases and Biomaterials (TBGS).

References

1. Darouiche RO. Device-associated infections: a macroproblem that starts with microadherence. Clin Infect Dis. 2001;33(9):1567–72.
2. An YH, Friedman RJ. Concise review of mechanisms of bacterial adhesion to biomaterial surfaces. J Biomed Mater Res. 1998;43:338–48.
3. DeMane CQ. The development of implants and implantable materials. Otolaryngol Clin North Am. 1995;28:225–34.
4. Zimmerli W, Trampuz A, Ochsner PE. Prosthetic-joint infections. N Engl J Med. 2004;351:1645–54.
5. Donlan RM. Biofilm formation: a clinically relevant microbiological process. Clin Infect Dis. 2001;33(8):1387–92.
6. Lew DP, Waldvogel FA. Osteomyelitis. N Engl J Med. 1997;336:999–1007.
7. Lowy FD. Staphylococcus aureus infections. N Engl J Med. 1998;339:520–32.
8. Sanderson PJ. Infection in orthopaedic implants. J Hosp Infect. 1991;18(Suppl A):367–75.
9. Goldsmith HL, Turitto VT. Rheological aspects of thrombosis and haemostasis: basic principles and applications. ICTH-report–subcommittee on rheology of the international committee on thrombosis and haemostasis. Thromb Haemost. 1986;55(3750272):415–35.
10. Katsikogianni M, Amanatides E, Mataras D, Missirlis YF. Staphylococcus epidermidis adhesion to He, He/O-2 plasma treated PET films and aged materials: contributions of surface free energy and shear rate. Colloid Surf B. 2008;65(2):257–68. doi:10.1016/j.colsurfb.2008.04.017.

11. Katsikogianni M, Spiliopoulou I, Dowling DP, Missirlis YF. Adhesion of slime producing *Staphylococcus epidermidis* strains to PVC and diamond-like carbon/silver/fluorinated coatings. J Mater Sci Mater Med. 2006;17:679–89.
12. Roosjen A, Boks NP, van der Mei HC, Busscher HJ, Norde W. Influence of shear on microbial adhesion to PEO-brushes and glass by convective-diffusion and sedimentation in a parallel plate flow chamber. Colloid Surf B. 2005;46(1):1–6. doi:10.1016/j.colsurtb.2005.08.009.
13. Mascari L, Ross JM. Hydrodynamic shear, collagen receptor density determine the adhesion capacity of S aureus to collagen. Ann Biomed Eng. 2001;29:956–62.
14. Anttila A, Lappalainen R, Heinonen H, Santavirta SS, Konttinen YT. Superiority of diamond like carbon coatings on articulating surfaces of artificial hip joints. New Diam Frontier Carbon Technol. 1999;9(4):283–8.
15. Lappalainen R, Anttila A, Heinonen H. Diamond coated total hip replacements. Clin Orthop Relat Res. 1998;352:118–27.
16. Lappalainen R, Selenius M, Anttila A, Konttinen YT, Santavirta SS. Reduction of wear in total hip replacement prostheses by amorphous diamond coatings. J Biomed Mater Res B. 2003;66:410–3.
17. Anttila A, Tiainen VM, Kiuru M, Alakoski E, Arstila K. Preparation of diamond-like carbon polymer hybrid films using filtered pulsed arc discharge method. Surf Eng. 2003;19(6):425–8.
18. Huikko K, Ostman P, Grigoras K, Tuomikoski S, Tiainen VM, Soininen A, et al. Poly(dimethylsiloxane) electrospray devices fabricated with diamond-like carbon-poly(dimethylsiloxane) coated SU-8 masters. Lab Chip. 2003;3:67–72.
19. Kiuru M, Alakoski E. Low sliding angles in hydrophobic and oleophobic coatings prepared with plasma discharge method. Mater Lett. 2004;58(16):2213–6.
20. Soininen A, Tiainen V-M, Konttinen YT, van der Mei HC, Busscher HJ, Sharma PK. Bacterial adhesion to diamond-like carbon as compared to stainless steel. J Biomed Mater Res B. 2009;90:882–5.
21. Anttila A. Structure-property relationships in surface-modified ceramics NATO ASI Series. Dordrecht: Kluwer; 1989.
22. Alakoski E, Kiuru M, Tiainen VM, Anttila A. Adhesion and quality test for tetrahedral amorphous carbon coating process. Diam Relat Mater. 2003;12(12):2115–8.
23. Anttila A, Hirvonen JP, Koskinen J Procedure and apparatus for the coating of materials by means of a pulsating plasma beam. US Patent patent US Patent No. 5078848 1992.
24. Anttila A, Salo J, Lappalainen R. High adhesion of diamond-like films achieved by the pulsed arc-discharge method. Mater Lett. 1995;24(1–3):153–6.
25. Lifshitz Y. Diamond-like carbon—present status. Diam Relat Mater. 1999;8(8–9):1659–76.
26. Robertson J. Diamond-like amorphous carbon. Mater Sci Eng R Rep. 2002;37(4–6):129–281.
27. Anttila A, Lappalainen R, Tiainen VM, Hakovirta M. Superior attachment of high-quality hydrogen-free amorphous diamond films to solid materials. Adv Mater. 1997;9(15):1161–4.
28. Valle J, Toledo-Arana A, Berasain C, Ghigo J-M, Amorena B, Penades JR, et al. SarA and not sigmaB is essential for biofilm development by *Staphylococcus aureus*. Mol Microbiol. 2003;48(12753197):1075–87.
29. Stavridi M, Katsikogianni M, Missirlis YF. The influence of surface patterning and/or sterilization on the haemocompatibility of polycaprolactones. Mat Sci Eng C. 2003;23(3):359–65.
30. Meinders JM, Vandermei HC, Busscher HJ. Insitu enumeration of bacterial adhesion in a parallel plate flow chamber—elimination or in focus flowing bacteria from the analysis. J Microbiol Meth. 1992;16(2):119–24.
31. Kinnari TJ, Soininen A, Esteban J, Zamora N, Alakoski E, Kouri V-P, et al. Adhesion of staphylococcal and Caco-2 cells on diamond-like carbon polymer hybrid coating. J Biomed Mater Res A. 2008;86(18041722):760–8.
32. Allen M, Myer B, Rushton N. In vitro and in vivo investigations into the biocompatibility of diamond-like carbon (DLC) coatings for orthopedic applications. J Biomed Mater Res. 2001;58(11319748):319–28.
33. Thomson LA, Law FC, Rushton N, Franks J. Biocompatibility of diamond-like carbon coating. Biomaterials. 1991;12(2009344):37–40.
34. Colas ACJ. Silicone biomaterials: history and chemistry. New York: Elsevier Inc.; 2004.
35. Teoh SHT ZG, Hastings GW. Handbook of biomaterial properties. London: Chapman & Hall; 1998.
36. McDonald JC, Whitesides GM. Poly(dimethylsiloxane) as a material for fabricating microfluidic devices. Acc Chem Res. 2002;35(12118988):491–9.
37. Shi L, Ardehali R, Caldwell KD, Valint P. Mucin coating on polymeric material surfaces to suppress bacterial adhesion. Colloid Surf B. 2000;17(4):229–39.
38. van Loosdrecht MC, Lyklema J, Norde W, Schraa G, Zehnder AJ. Electrophoretic mobility and hydrophobicity as a measured to predict the initial steps of bacterial adhesion. Appl Environ Microbiol. 1987;53:1898–901.
39. Cerca N, Pier GB, Vilanova M, Oliveira R, Azeredo J. Quantitative analysis of adhesion and biofilm formation on hydrophilic and hydrophobic surfaces of clinical isolates of *Staphylococcus epidermidis*. Res Microbiol. 2005;156(15862449):506–14.
40. Shin YN, Kim BS, Ahn HH, Lee JH, Kim KS, Lee JY, et al. Adhesion comparison of human bone marrow stem cells on a gradient wettable surface prepared by corona treatment. Appl Surf Sci. 2008;255:293–6. doi:10.1016/j.apsusc.2008.06.173.
41. Raulio M, Jarn M, Ahola J, Peltonen J, Rosenholm JB, Tervakangas S, et al. Microbe repelling coated stainless steel analysed by field emission scanning electron microscopy and physicochemical methods. J Ind Microbiol Biotechnol. 2008;35:751–60.
42. Jones DS, Garvin CP, Dowling D, Donnelly K, Gorman SP. Examination of surface properties and in vitro biological performance of amorphous diamond-like carbon-coated polyurethane. J Biomed Mater Res B. 2006;78B(2):230–6. doi:10.1002/Jbm.B.30474.
43. Palmer J, Flint S, Brooks J. Bacterial cell attachment, the beginning of a biofilm. J Ind Microbiol Biot. 2007;34(9):577–88. doi:10.1007/s10295-007-0234-4.
44. Levon J, Myllymaa K, Kouri VP, Rautemaa R, Kinnari T, Myllymaa S, et al. Patterned macroarray plates in comparison of bacterial adhesion inhibition of tantalum, titanium, and chromium compared with diamond-like carbon. J Biomed Mater Res A. 2010;92A(4):1606–13. doi:10.1002/Jbm.A.32486.
45. Chen W, Fadeev AY, Hsieh MC, Oner D, Youngblood J, McCarthy TJ. Ultrahydrophobic and ultralyophobic surfaces: Some comments and examples. Langmuir. 1999;15(10):3395–9.
46. Hilbert LR, Bagge-Ravn D, Kold J, Gram L. Influence of surface roughness of stainless steel on microbial adhesion and corrosion resistance. Int Biodeter Biodegr. 2003;52(3):175–85. doi:10.1016/S0964-8305(03)00104-5.
47. Taylor RL, Verran J, Lees GC, Ward AJ. The influence of substratum topography on bacterial adhesion to polymethyl methacrylate. J Mater Sci Mater Med. 1998;9:17–22.